CRYSTAL GROWTH & DESIGN

pubs.acs.org/crystal

Article

Symmetry-Dependent Intermolecular $\pi-\pi$ Stacking Directed by Hydrogen Bonding in Racemic Copper-Phenanthroline Compounds

Matthew L. Nisbet, Yiran Wang, and Kenneth R. Poeppelmeier*

Cite This: *Cryst. Growth Des.* 2021, 21, 552–562

Read Online

ACCESS | Metrics & More | Article Recommendations | Supporting Information

ABSTRACT: We examine the role of molecular symmetry and hydrogen bonding in determining heterochiral intermolecular $\pi-\pi$ stacking motifs in four racemic compounds with the formula $[Cu(phen)_2(H_2O)][MF_6]\cdot xH_2O$ (M = Ti, Zr, Hf; phen = 1,10-phenanthroline) and two racemic compounds with the formula $Cu(phen)_2MF_6\cdot H_2O$ (M = Zr, Hf). In this work, equimolar combinations of C_2-symmetric Δ- and Λ-$Cu(phen)_2(H_2O)^{2+}$ complexes were found to organize via only face-to-face $\pi-\pi$ stacking interactions to adopt a new horizontal packing motif in a series of compounds with the formula $[Cu(phen)_2(H_2O)][MF_6]\cdot xH_2O$ (M = Ti, Zr, Hf). Previously, Δ- and Λ-$Cu(phen)_2(H_2O)^{2+}$ complexes had been observed to pack with only parallel displaced $\pi-\pi$ stacking interactions in a diagonal packing motif or with both face-to-face and parallel displaced $\pi-\pi$ stacking interactions in a zigzag packing motif. The horizontal arrangement reported here is associated with the formation of hydrogen-bonding networks that link cations, anions, and hydrating water molecules within these structures. Equimolar combinations of neutral Δ- and Λ-$Cu(phen)_2MF_6$ (M = Zr, Hf) molecules organize in a zigzag stacking pattern that originates from the presence of both parallel displaced and face-to-face $\pi-\pi$ stacking interactions. The symmetry of the $Cu(phen)_2MF_6$ molecule is reduced to C_1 by tilting of the bound MF_6^{2-} octahedron, which renders the two phen ligands symmetrically inequivalent.

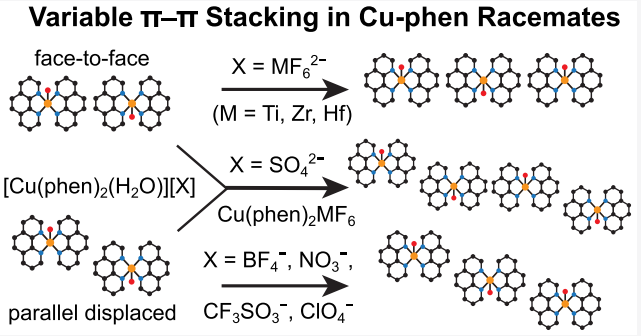

INTRODUCTION

Noncovalent interactions such as $\pi-\pi$ stacking and hydrogen bonding play a key role in determining structure, properties, and intermolecular symmetry in many systems.[1−7] In the design of noncentrosymmetric (NCS) materials, these interactions often dictate the presence or absence of inversion symmetry, which in turn determines the nonlinear optical activity, piezoelectricity, and other properties.[8−10] The synthesis of NCS materials focuses on controlling the alignment of acentric functional building units (FBUs), such as polar early-transition-metal (ETM) octahedra, conjugated planar groups, and tetrahedra.[11] Isolated ETM fluorides and oxide fluorides can be synthesized in concentrated HF, which gives improved synthetic control over the environment of these anions to optimize structure and properties in NCS structures.[12] The introduction of enantiomerically pure chiral templating agents (CTAs) ensures inversion symmetry breaking, but this method is limited by the requirement for enantiomeric purification.[13] Further, such a strategy does not control the cooperative polar alignment of FBUs, meaning that improved synthetic methods must be developed to precisely control the alignment of chiral and polar FBUs with noncovalent interactions.[14−18]

The use of racemic mixtures, or equimolar combinations of both enantiomers, of CTAs has been demonstrated as an emerging strategy for the synthesis of NCS materials.[19−21] While enantiomerically pure reagents require tedious separation and purification,[13,22,23] racemic mixtures of chiral molecules may be easily generated *in situ*. Notably, equimolar combinations of Δ- and Λ-$Cu(bpy)_2(H_2O)^{2+}$ complexes cooperatively align the polar moments of MF_6^{2-} (M = Ti, Zr, Hf; bpy = 2,2′-bipyridine) octahedra, which undergo polarizing out-of-center distortions owing to second-order Jahn−Teller effects.[21,24,25] Although most racemates crystallize with inversion symmetry and the chemical origins of inversion symmetry breaking in racemic compounds remain unclear, previous studies of materials based on ETM octahedra and chiral Δ- and Λ-$M(bpy)_x(H_2O)_y$ (M = Cu, Ni, Zn; x = 2, 3; y = 0, 1, 2) coordination complexes indicate that the racemic $[Cu(bpy)_2(H_2O)][MF_6]$ compounds possess a unique combination of cation symmetry and hydrogen-bonding networks that give rise to polar NCS structures.[21,26] However, whereas the $[Cu(bpy)_2(H_2O)][MF_6]$ (M = Ti, Zr, Hf) compounds

Received: September 30, 2020
Revised: November 18, 2020
Published: December 1, 2020

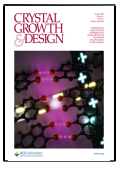

https://dx.doi.org/10.1021/acs.cgd.0c01355
Cryst. Growth Des. 2021, 21, 552–562

Table 1. Crystallographic Data for Compounds 1 and 2

	compound 1	compound 2
empirical formula	$C_{24}H_{20}CuF_6N_4O_2Ti$	$C_{24}H_{18}CuF_6N_4OHf$
formula wt	621.88	734.45
temp/K	99.99	100.04
cryst syst	monoclinic	triclinic
space group	$C2/c$	$P\bar{1}$
a, Å	19.6498(3)	12.6902(17)
b, Å	16.7910(2)	14.2854(19)
c, Å	14.0998(2)	16.910(2)
α, deg	90	88.959(6)
β, deg	95.7300(10)	70.804(6)
γ, deg	90	67.426(6)
volume, Å^3	4628.84(11)	2652.6(6)
Z	8	4
ρ_{calcd}, g/cm^3	1.785	1.839
μ, mm^{-1}	1.345	4.778
$F(000)$	2504	1412
cryst size, mm^3	0.11 × 0.081 × 0.056	0.198 × 0.149 × 0.11
radiation	Mo Kα (λ = 0.71073 Å)	Mo Kα (λ = 0.71073 Å)
2θ range for data collection, deg	3.198−61.188	2.57−62.006
index ranges	$-28 \le h \le 26$, $-24 \le k \le 23$, $-20 \le l \le 19$	$-18 \le h \le 18$, $-20 \le k \le 20$, $-24 \le l \le 24$
no. of rflns collected	27520	193041
no. of indep rflns	7129 (R_{int} = 0.0430, R_{sigma} = 0.0404)	16583 (R_{int} = 0.0361, R_{sigma} = 0.0156)
no. of data/restraints/params	7129/0/359	16583/0/703
goodness of fit on F^2	1.028	1.044
final R indexes ($I \ge 2\sigma(I)$)	R_1 = 0.0383, wR_2 = 0.0948	R_1 = 0.0296, wR_2 = 0.0658
final R indexes (all data)	R_1 = 0.0513, wR_2 = 0.1012	R_1 = 0.0315, wR_2 = 0.0669
largest diff peak/hole, e Å^{-3}	0.60/−0.78	3.38/−5.97

form polar NCS structures, centrosymmetry is always observed in the case of racemic Cu-phen compounds reported here.

Here, we elucidate the role of intermolecular $\pi-\pi$ interactions in breaking inversion symmetry in racemic compounds by comparing the differences in $\pi-\pi$ stacking between analogous complexes with bpy and phen ligands. Intermolecular $\pi-\pi$ stacking interactions can be understood in terms of four principal components: repulsion, induction, dispersion, and electrostatic interactions.[27,28] An examination of $\pi-\pi$ stacking interactions in square-planar metal complexes of 2,2′-bipyridine and 1,10-phenanthroline via both a statistical analysis of observed stacking geometries and density functional theory calculations revealed that the strength of the stacking interaction increases as the surface area overlap increases when these ligands are bound to metal atoms.[29,30] However, factors such as the steric bulk of other ligands and other strong interactions in the structure often lead to geometries other than the most stable $\pi-\pi$ stacking configuration being observed.

We report the structures of four racemic compounds based on Δ- and Λ-Cu(phen)$_2$(H$_2$O)$^{2+}$ cations and the ETM fluoride MF$_6^{2-}$ (M = Ti, Zr, Hf) anions and two racemic compounds based on neutral bridged Λ-shaped Δ- and Λ-Cu(phen)$_2$(MF$_6$) (M = Zr, Hf) complexes. The [Cu(phen)$_2$(H$_2$O)][MF$_6$] (M = Ti, Zr, Hf) compounds represent the first examples of C_2-symmetric Δ- and Λ-Cu(phen)$_2$(H$_2$O)$^{2+}$ units arranged exclusively by face-to-face stacking interactions to adopt a horizontal stacking pattern. This novel stacking motif occurs in the presence of extended hydrogen-bonding networks among cations, anions, and free water molecules. Previously, only diagonal and zigzag arrangements had been observed, which are associated with the presence of only parallel displaced or both parallel displaced and face-to-face stacking, respectively. Structures with only parallel displaced stacking geometries are observed in the presence of singly charged anions, which do not allow for the formation of extended hydrogen-bonding networks, as seen in [Cu(phen)$_2$(H$_2$O)][X]$_2$, where X = BF$_4^-$, NO$_3^-$, CF$_3$SO$_3^-$, ClO$_4^-$.[31−33] Zigzag stacking occurs when both parallel displaced and face-to-face geometries are present in the same structure, which occurs in the two Cu(phen)$_2$MF$_6$·H$_2$O (M = Zr, Hf) compounds reported here, as well as in the known compounds [Cu(phen)$_2$(H$_2$O)][SO$_4$]·4H$_2$O and [Cu(phen)$_2$(SO$_4$)](H$_2$O)$_2$(dmf).[9] In these structures, the symmetry of the chiral copper(II) complex is reduced from C_2 to C_1 by the tilting of the apical ligand,

By comparing the structures of the racemic compounds reported in this work with those of the known compounds based on Δ- and Λ-Cu(phen)$_2$(H$_2$O)$^{2+}$ and Δ- and Λ-Cu(bpy)$_2$(H$_2$O)$^{2+}$ complexes, we identify the importance of nonparallel stacking between bpy ligands as a necessary, albeit insufficient, factor in breaking inversion symmetry within the bulk structure.

METHODS

Caution! Hydrofluoric acid (HF) is toxic and corrosive! HF must be handled with extreme caution and the appropriate protective gear.

Materials. TiO$_2$ (Aldrich, 99.9+%), ZrO$_2$ (Alfa Aesar, 99.978%), HfO$_2$ (Aldrich, 98%), CuO (Sigma-Aldrich, ≥99.0%), 1,10-phenanthroline (phen) (Fisher, 99%), and HF(aq) (Sigma-Aldrich, 48 wt % in H$_2$O, ≥99.99+% trace metals basis) were used as received. Reagent amounts of deionized water were used.

Hydrothermal Synthesis. The compounds reported here were synthesized via the hydrothermal pouch method.[34] In each reaction,

https://dx.doi.org/10.1021/acs.cgd.0c01355
Cryst. Growth Des. 2021, 21, 552−562

Table 2. Crystallographic Data for Compounds 3 and 4

	compound **3**	compound **4**
empirical formula	$C_{24}H_{18}CuF_6N_4O_{1.64}Zr$	$C_{24}H_{18}CuF_6N_4O_{1.87}Hf$
formula wt	657.34	748.33
temp, K	100	100.01(10)
cryst syst	monoclinic	monoclinic
space group	*P*2/*n*	*P*2/*n*
a, Å	11.6643(7)	11.7715(3)
b, Å	16.9423(10)	16.9235(3)
c, Å	12.8320(7)	12.8110(3)
α, deg	90	90
β, deg	109.6293(10)	109.839(3)
γ, deg	90	90
volume, Å^3	2388.5(2)	2400.67(10)
Z	4	4
ρ_{calcd}, g/cm^3	1.828	2.070
μ, mm^{-1}	1.403	5.284
F(000)	1304	1440
cryst size, mm^3	0.359 × 0.208 × 0.162	0.287 × 0.182 × 0.139
radiation	Mo K*α* (*λ* = 0.71073 Å)	Mo K*α* (*λ* = 0.71073 Å)
2*θ* range for data collection, deg	2.404−59.176	4.064−67.708
index ranges	$-15 \le h \le 16, -22 \le k \le 23, -16 \le l \le 17$	$-18 \le h \le 16, -25 \le k \le 24, -19 \le l \le 18$
no. of rflns collected	26104	36266
no. of indep rflns	6698 (R_{int} = 0.0368, R_{sigma} = 0.0350)	8504 (R_{int} = 0.0339, R_{sigma} = 0.0329)
no. of data/restraints/params	6698/0/417	8504/4/401
goodness of fit on F^2	1.030	1.046
final *R* indexes ($I \ge 2\sigma(I)$)	R_1 = 0.0344, wR_2 = 0.0821	R_1 = 0.0341, wR_2 = 0.0857
final *R* indexes (all data)	R_1 = 0.0482, wR_2 = 0.0883	R_1 = 0.0444, wR_2 = 0.0903
largest diff peak/hole, e Å^{-3}	0.54/−0.78	2.24/−1.99

Table 3. Crystallographic Data for Compounds 5 and 6

	compound **5**	compound **6**
empirical formula	$C_{24}H_{16}CuF_6N_4OZr$	$C_{24}H_{16}CuF_6N_4OHf$
formula wt	645.17	732.44
temp, K	100.04	99.99
cryst syst	monoclinic	monoclinic
space group	$P2_1/n$	$P2_1/n$
a, Å	8.4159(2)	8.4064(10)
b, Å	14.3659(5)	14.3531(18)
c, Å	18.2917(6)	18.264(2)
α, deg	90	90
β, deg	99.9720(10)	99.946(3)
γ, deg	90	90
volume, Å^3	2178.09(12)	2170.5(5)
Z	4	4
ρ_{calcd}, g/cm^3	1.967	2.241
μ, mm^{-1}	1.535	5.839
F(000)	1276	1404
cryst size, mm^3	0.116 × 0.107 × 0.1	0.398 × 0.332 × 0.332
radiation	Mo K*α* (*λ* = 0.71073 Å)	MoK*α* (*λ* = 0.71073 Å)
2*θ* range for data collection, deg	3.626−61.13	3.63−63.202
index ranges	$-12 \le h \le 11, -18 \le k \le 20, -26 \le l \le 26$	$-12 \le h \le 8, -12 \le k \le 21, -19 \le l \le 26$
no. of rflns collected	19983	20665
no. of indep rflns	6649 (R_{int} = 0.0234, R_{sigma} = 0.0250)	7255 (R_{int} = 0.0134, R_{sigma} = 0.0145)
no. of data/restraints/params	6649/0/334	7255/0/334
goodness of fit on F^2	1.034	1.169
final *R* indexes ($I \ge 2\sigma(I)$)	R_1 = 0.0229, wR_2 = 0.0599	R_1 = 0.0178, wR_2 = 0.0390
final *R* indexes (all data)	R_1 = 0.0250, wR_2 = 0.0609	R_1 = 0.0198, wR_2 = 0.0395
largest diff peak/hole, e Å^{-3}	0.52/-0.67	0.63/-1.08

reagents were heat-sealed in Teflon pouches. Groups of six pouches were then placed into 125 mL Parr autoclaves with 40 mL of distilled water as backfill. The autoclaves were heated at a rate of 5 °C/min to 150 °C and held at 150 °C for 24 h. The autoclaves were cooled to

https://dx.doi.org/10.1021/acs.cgd.0c01355
Cryst. Growth Des. 2021, 21, 552−562

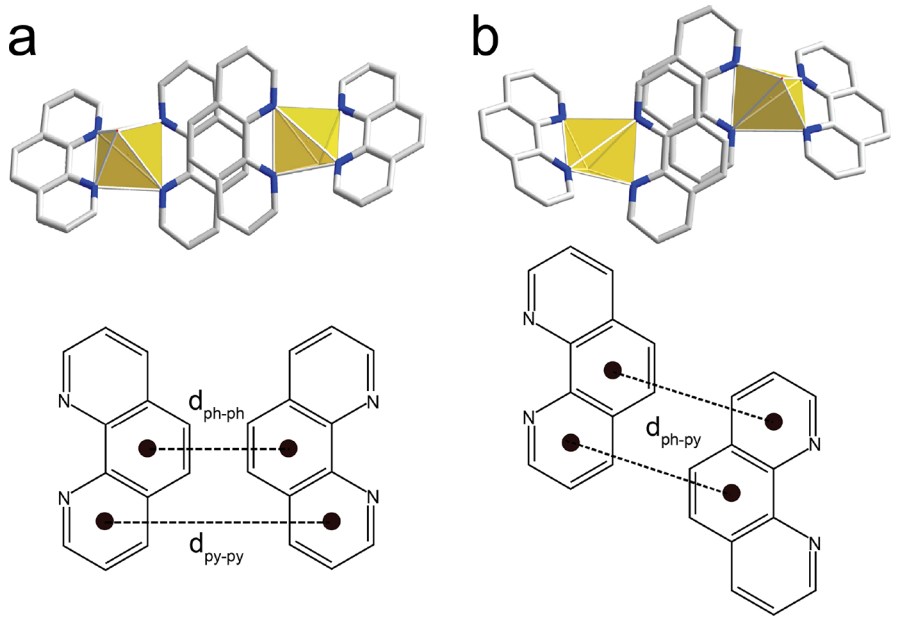

Figure 1. (a) Representative face-to-face $\pi-\pi$ stacking interaction between adjacent $Cu(phen)_2(H_2O)^{2+}$ cations. Interactions of this type can be identified by short d_{ph-ph} distances. (b) Representative parallel displaced $\pi-\pi$ stacking interaction between adjacent $Cu(phen)_2(H_2O)^{2+}$ cations. Interactions of this type can be identified by short d_{ph-py} distances.

room temperature at a rate of 6 °C/h. Solid products were recovered by vacuum filtration.

Compound **1**, $[Cu(phen)_2(H_2O)][TiF_6]\cdot H_2O$, was synthesized in a Teflon pouch containing 1.69 mmol of CuO, 1.69 mmol of TiO_2, 2.56 mmol of phen, 1.0 mL (27.6 mmol) of HF(aq), and 0.1 mL (5.6 mmol) of H_2O.

Compound **2**, $[Cu(phen)_2(H_2O)]_2[HfF_6]_2\cdot xH_2O$, was synthesized in a Teflon pouch containing 1.69 mmol of CuO, 1.69 mmol of HfO_2, 7.68 mmol of phen, 1.0 mL (27.6 mmol) of HF(aq), and 0.1 mL (5.6 mmol) of H_2O.

Compound **3**, $[Cu(phen)_2(H_2O)][ZrF_6]\cdot 0.64H_2O$, was synthesized in a Teflon pouch containing 1.69 mmol of CuO, 1.69 mmol of ZrO_2, 2.56 mmol of phen, 0.4 mL (11.0 mmol) of HF(aq), and 0.7 mL (38.9 mmol) of H_2O.

Compound **4**, $[Cu(phen)_2(H_2O)][HfF_6]\cdot 0.87H_2O$, was synthesized in a Teflon pouch containing 1.69 mmol of CuO, 1.69 mmol of HfO_2, 2.56 mmol of phen, 0.2 mL (5.5 mmol) of HF(aq), and 0.9 mL (50.0 mmol) of H_2O.

Compound **5**, $Cu(phen)_2ZrF_6\cdot H_2O$, was synthesized in a Teflon pouch containing 1.69 mmol of CuO, 1.69 mmol of ZrO_2, 5.12 mmol of phen, 1.0 mL (27.6 mmol) of HF(aq), and 0.1 mL (5.5 mmol) of H_2O.

Compound **6**, $Cu(phen)_2HfF_6\cdot H_2O$, was synthesized in a Teflon pouch containing 1.69 mmol of CuO, 1.69 mmol of HfO_2, 2.56 mmol of phen, 0.8 mL (22.1 mmol) of HF(aq), and 0.3 mL (16.7 mmol) of H_2O.

Single-Crystal X-ray Diffraction. Single-crystal X-ray diffraction was used to determine the structure of each reported compound. Diffraction data for compounds **1**−**3**, **5**, and **6** were recorded on Bruker-APEX II CCD diffractometers at 100 K with monochromated Mo Kα radiation (λ = 0.71073 Å). SAINT was used for integration, and multiscan absorption corrections were applied with SADABS.[35,36]

Diffraction data for compound **4** were recorded at 100 K on a Rigaku XtaLAB Synergy HyPix diffractometer with monochromated Mo Kα radiation (λ = 0.71073 Å). CrysAlisPro 1.171.40.68a was used for integration and scaling of the data.[37] A numerical absorption correction was applied on the basis of Gaussian integration over a multifaceted crystal model with an empirical absorption correction using spherical harmonics, as implemented in the SCALE3 ABSPACK scaling algorithm.

All structures were solved with SHELXT and refined with SHELXL.[38] Hydrogen atom positions were assigned from difference map peaks where possible and omitted otherwise, with the exception of the hydrogen atoms of 1,10-phenanthroline, which were constrained to ride at distances of 0.93 Å from the associated C atoms with $U_{iso}(H) = 1.5U_{eq}(C)$ within Olex2.[39] In cases where both hydrogen atoms of free water molecules could not be determined, we have reported only the oxygen atom position. No additional symmetry was found in checking for higher symmetry using PLATON.[40] Crystallographic data for compounds **1**−**6** are given in Tables 1−3.

Descriptors for Intermolecular Interactions. Pairwise centroid−centroid distances were calculated for each pair of rings in adjacent phen ligands (e.g., phenyl−phenyl (d_{ph-ph}), pyridine−phenyl (d_{py-ph}), and pyridine−pyridine (d_{py-py}))[9] to classify $\pi-\pi$ stacking arrangements between $Cu(phen)_2(H_2O)^{2+}$ or $Cu(phen)_2(MF_6)$ (M = Zr, Hf) fragments as either face-to-face or parallel displaced. The shorter distance is reported for structures with multiple values of d_{py-py} and d_{ph-py}. Figure 1 depicts representative face-to-face and parallel displaced interactions. Calculated centroid−centroid distances can be found in Table 4. A full listing of calculated descriptors for compounds **1**−**6** and the known compounds $Cu(phen)_2(H_2O)^{2+}$ and $Cu(bpy)_2(H_2O)^{2+}$ is given in Table 4 and Tables S1 and S2. We note that the measured interplanar distances between bpy and phen ligands fall within the range 3.3−3.76 Å, which is near the center of the distribution of known interplanar distances in bpy and phen metal complexes.[29,30] The packing motif of a structure is assigned as horizontal if only face-to-face interactions are present, zigzag if both face-to-face and parallel displaced stacking interactions are present, and diagonal if only parallel displaced stacking interactions are present. A general schematic of the horizontal, zigzag, and diagonal packing motifs is shown in Figure S1.

Descriptors for hydrogen-bonding interactions in compounds **1**−**6** are provided in Table 5. A search of O−H···F interactions among entries in the Cambridge Structural Database reveals an average O−F distance of 2.788 Å and a median distance of 2.802 Å.[41]

RESULTS AND DISCUSSION

Structure Descriptions. An examination of the three (CuO, MO_2)/phen/HF(aq) (M = Ti, Zr, Hf) systems revealed four compounds based on racemic combinations of chiral Δ- and Λ-$Cu(phen)_2(H_2O)^{2+}$ cations.

https://dx.doi.org/10.1021/acs.cgd.0c01355
Cryst. Growth Des. 2021, 21, 552−562

Table 4. Heterochiral Stacking Interaction Descriptors for Compounds 1−6[a]

compound	d_{ph-py}, Å	d_{py-py}, Å	d_{ph-ph}, Å	stacking type
1	3.7195(11)	4.2989(10)	**3.5112(10)**	face-to-face
	4.1429(11)	4.7265(11)	**3.5269(11)**	face-to-face
2	3.9877(17)	4.4328(16)	**3.5109(16)**	face-to-face
	3.8039(18)	4.6337(18)	**3.6242(17)**	face-to-face
3	3.9089(15)	4.4715(14)	**3.5123(14)**	face-to-face
	3.8695(13)	4.5123(13)	**3.5130(13)**	face-to-face
4	3.917(2)	4.459(2)	**3.507(2)**	face-to-face
	3.893(2)	4.536(2)	**3.523(2)**	face-to-face
5	3.7884(8)	3.7286(8)	**3.5527(8)**	face-to-face
	3.6019(8)	**3.7109(8)**	4.3379(8)	parallel displaced
6	3.7844(11)	3.7217(11)	**3.5508(11)**	face-to-face
	3.5976(11)	**3.7051(11)**	4.3306(11)	parallel displaced

[a]Two distinct stacking interactions were observed for each structure. The distances used to classify each phen−phen interaction are given in boldface for emphasis.

Compound **1** has the formula $[Cu(phen)_2(H_2O)][TiF_6]\cdot H_2O$ and crystallizes in the space group $C2/c$. The structure of compound **1** contains racemic combinations of C_2-symmetric Δ- and Λ-$Cu(phen)_2(H_2O)^{2+}$ complexes, which are organized into layers that stack along the b axis by homochiral and heterochiral $\pi-\pi$ stacking interactions as well as hydrogen bonding with TiF_6^{2-} anions (Figure 2a). Adjacent layers of Δ- and Λ-$Cu(phen)_2(H_2O)^{2+}$ complexes are aligned in register such that parallel rows of Δ- and Λ-$Cu(phen)_2(H_2O)^{2+}$ complexes form along a. Each TiF_6^{2-} anion participates in hydrogen bonding with two $Cu(phen)_2(H_2O)^{2+}$ units of the same handedness and the free water molecule located between layers of $Cu(phen)_2(H_2O)^{2+}$ units. Two distinct face-to-face heterochiral stacking contacts are observed. These heterochiral stacking interactions result in the formation of extended Δu−Λd−Δu−Λd and Δd−Λu−Δd−Λu chains (u = up and d = down describe the orientation of these cations along the b direction). These stacking chains in which cations alternate in orientation and chirality have been shown to allow for optimal near-parallel stacking, while other arrangements with a single chirality or orientation give less favorable stacking interactions.[21] Homochiral $\pi-\pi$ stacking between chains results in the formation of Δ−Δ and Λ−Λ dimers, which display nonparallel stacking of both phen ligands bound to adjacent $Cu(phen)_2(H_2O)^{2+}$ complexes (Figure 2b). For the homochiral stacking interactions, one pair of phen ligands stacks in a face-to-face arrangement, while the other pair stacks in a displaced fashion.

Compound **2** has the formula $[Cu(phen)_2(H_2O)][HfF_6]\cdot xH_2O$ and crystallizes in the space group $P\bar{1}$. The structure is analogous to the structure of **1** in that it contains racemic combinations of Δ- and Λ-$Cu(phen)_2(H_2O)^{2+}$ arranged into Δu−Λd−Δu−Λd and Δd−Λu−Δd−Λu chains and Δ−Δ and Λ−Λ dimers via $\pi-\pi$ stacking and hydrogen bonding (Figure 3). Whereas the layers of Δ- and Λ-$Cu(phen)_2(H_2O)^{2+}$ are aligned to form parallel rows of Δ- and Λ-$Cu(phen)_2(H_2O)^{2+}$ complexes in compound **1**, adjacent layers are shifted along c in an offset fashion in compound **2** to give an alternating "brickwork" arrangement. Two distinct HfF_6^{2-} anions are present in the asymmetric unit. Each HfF_6^{2-} anion participates in two hydrogen bonds with two $Cu(phen)_2(H_2O)^{2+}$ units of the same handedness. The $Hf(2)F_6^{2-}$ anion displays disorder on the F11 and F12 sites. A solvent mask was applied during

Table 5. Hydrogen-Bonding Interactions in Compounds 1−6

D	H	A	d(D−H), Å	d(H−A), Å	d(D-A), Å	D−H−A, deg
			Compound **1**			
O1	H1A	F1	0.79(3)	1.79(4)	2.574(2)	170(3)
O1	H1B	F3	0.80(3)	1.82(3)	2.619(2)	176(3)
O2	H2A	F4	0.97(4)	1.81(4)	2.755(2)	162(3)
			Compound **2**			
O1	H1A	F8	0.70(6)	1.90(6)	2.602(3)	175(6)
O1	H1B	F1	0.75(5)	1.90(5)	2.643(3)	172(5)
O2	H2A	F10	0.76(5)	1.89(5)	2.655(3)	175(5)
O2	H2B	F3	0.74(5)	1.90(5)	2.638(3)	171(5)
			Compound **3**			
O1	H1A	F3B	0.75(3)	1.72(4)	2.470(5)	171(3)
O1	H1A	F3A	0.75(3)	1.98(4)	2.695(7)	160(3)
O1	H1B	F2B	0.70(3)	2.02(4)	2.72(3)	177(3)
O1	H1B	F2A	0.70(3)	1.77(4)	2.46(2)	168(4)
O2		F6A			2.724(5)	
O3		F5B			2.59(6)	
			Compound **4**			
O1	H1A	F4A	0.843(19)	1.69(2)	2.499(7)	161(5)
O1	H1A	F4B	0.843(19)	1.90(2)	2.722(12)	164(4)
O1	H1B	F1	0.817(19)	1.784(19)	2.598(4)	174(4)
O2		F6B			2.716(7)	
O3		F3A			2.661(12)	
			Compound **5**			
O1		F2			2.4454(16)	
			Compound **6**			
O1		F2			2.442(2)	

https://dx.doi.org/10.1021/acs.cgd.0c01355
Cryst. Growth Des. 2021, 21, 552−562

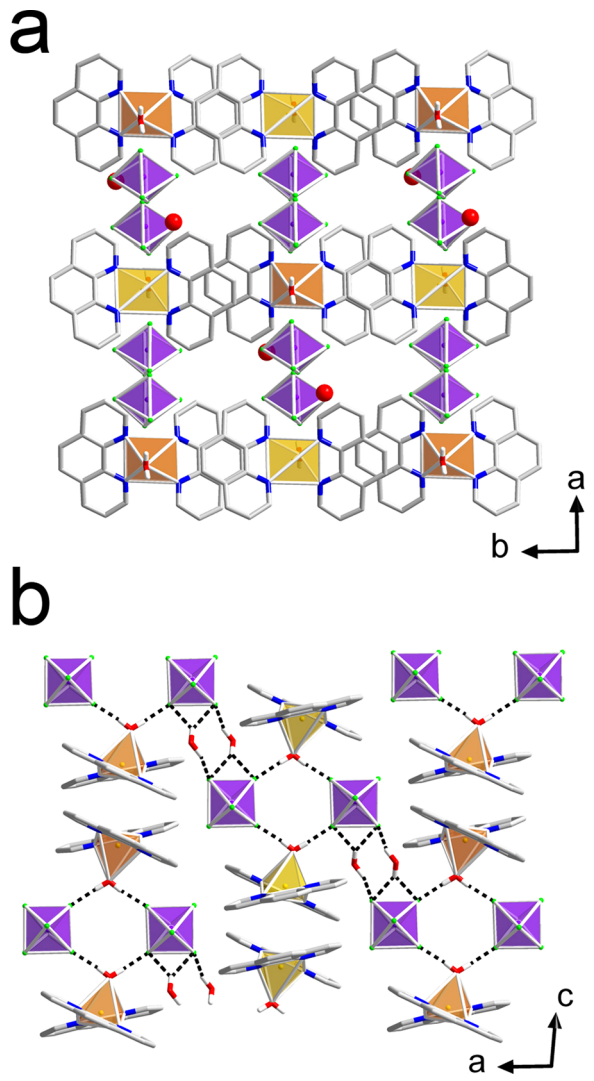

Figure 2. (a) Structural diagram showing the face-to-face stacking interactions in the structure of compound **1**. (b) Hydrogen bonds within the structure are depicted as dashed lines. Orange polyhedra represent Λ-Cu(phen)$_2$(H$_2$O)$^{2+}$ cations, gold polyhedra represent Δ-Cu(phen)$_2$(H$_2$O)$^{2+}$ cations, and purple polyhedra represent TiF$_6^{2-}$ anions.

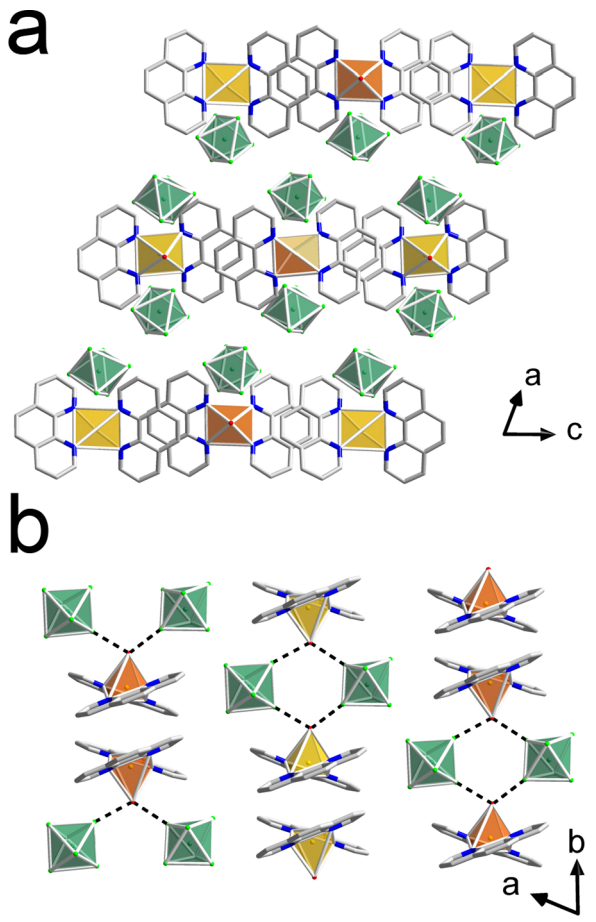

Figure 3. (a) Structural diagram showing the face-to-face stacking interactions in the structure of compound **2**. (b) Hydrogen bonds within the structure are depicted as dashed lines. Orange polyhedra represent Λ-Cu(phen)$_2$(H$_2$O)$^{2+}$ cations, gold polyhedra represent Δ-Cu(phen)$_2$(H$_2$O)$^{2+}$ cations, and green polyhedra represent HfF$_6^{2-}$ anions.

the refinement to model disordered free water molecules present in the structure. These free water molecules are packed between the hydrogen-bonded layers of Cu(phen)$_2$(H$_2$O)$^{2+}$ and HfF$_6^{2-}$ units. Compound **2** contains two types of heterochiral face-to-face stacking interactions. Both homochiral stacking interactions exhibit a displaced arrangement.

Compound **3** has the formula [Cu(phen)$_2$(H$_2$O)][ZrF$_6$]·0.64H$_2$O and crystallizes in the space group *P*2/*n*. Hydrogen bonding and $\pi-\pi$ stacking interactions dictate the assembly of Cu(phen)$_2$(H$_2$O)$^{2+}$ and ZrF$_6^{2-}$ units within the structure of **3** into both Δu−Λd−Δu−Λd and Δd−Λu−Δd−Λu chains and Δ−Δ and Λ−Λ dimers (Figure 4). Layers of Δ- and Λ-Cu(phen)$_2$(H$_2$O)$^{2+}$ complexes are aligned in register, as seen in compound **1**. Disorder is present at three F sites in the ZrF$_6^{2-}$ octahedron. In this structure, the ZrF$_6^{2-}$ anions participate in two hydrogen bonds with Cu(phen)$_2$(H$_2$O)$^{2+}$ units of the same handedness and two hydrogen bonds with free water molecules. The free O2 water molecule is fully occupied, while the free O3 water molecule has a partial occupancy of 0.14. Two distinct heterochiral stacking interactions with face-to-face configurations are observed within Δu−Λd−Δu−Λd and Δd−Λu−Δd−Λu chains in **3**. The homochiral stacking interactions include one face-to-face contact and one slightly displaced contact.

Compound **4** has the formula [Cu(phen)$_2$(H$_2$O)][HfF$_6$]·0.87H$_2$O and is isostructural with compound **3** with the exception of the difference in occupancy of the free O3 water molecule, which has a partial occupancy of 0.37 in compound **4**.

In addition to the four racemic compounds based on Cu(phen)$_2$(H$_2$O)$^{2+}$ cations, our investigation also produced two isostructural racemates with the formula Cu(phen)$_2$MF$_6$·H$_2$O (M = Zr, Hf) in which the MF$_6^{2-}$ octahedron is directly bound in the apical site of the neutral Δ- and Λ-Cu(phen)$_2$MF$_6$ complexes.

Compound **5** has the formula Cu(phen)$_2$ZrF$_6$·H$_2$O and crystallizes in the space group *P*2$_1$/*n*. The structure of **5** contains racemic combinations of Δ- and Λ-Cu(phen)$_2$ZrF$_6$ units, which adopt bent Λ-shaped configurations, and a free water molecule (Figure 5).[42] Each Cu(phen)$_2$ZrF$_6$ unit participates in hydrogen bonding with a free water molecule. Cu(phen)$_2$ZrF$_6$ units are involved in face-to-face and parallel displaced heterochiral stacking interactions and form Δu−Λd−Δu−Λd chains. Notably, the apical ZrF$_6^{2-}$ octahe-

https://dx.doi.org/10.1021/acs.cgd.0c01355
Cryst. Growth Des. 2021, 21, 552−562

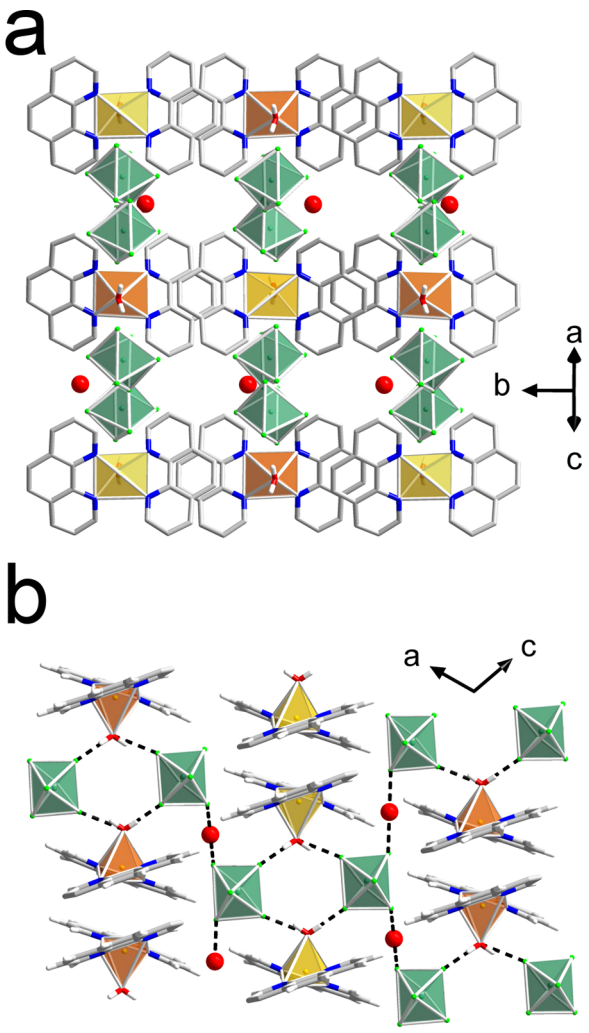

Figure 4. (a) Structural diagram showing the face-to-face stacking interactions in the structure of compounds **3** and **4**. (b) Hydrogen bonds within the structure are depicted as dashed lines. Orange polyhedra represent Λ-Cu(phen)$_2$(H$_2$O)$^{2+}$ cations, gold polyhedra represent Δ-Cu(phen)$_2$(H$_2$O)$^{2+}$ cations, and green polyhedra represent HfF$_6^{2-}$ anions.

dron is tilted toward the phenanthroline ligand that participates in a face-to-face stacking interaction (Figure S2). Homochiral stacking is absent from the structure, and thus Δ−Δ and Λ−Λ dimers do not form. Previous studies of stacking in square-planar metal complexes of phen indicate that the formation of $\pi-\pi$ stacking chains, in which each phen ligand participates in two stacking interactions, is heavily favored over stacking dimers, in which each phen ligand participates in only one stacking interaction, in known structures. However, in compound **5**, the steric bulk of the bound MF$_6^{2-}$ octahedron disrupts the stacking landscape such that each phen ligand only participates in one stacking interaction.

Compound **6** has the formula Cu(phen)$_2$HfF$_6$·H$_2$O and is isostructural with compound **5**.

$\pi-\pi$ Stacking Motifs in Racemic Copper-Phenanthroline Compounds. In addition to the structures reported above, we examined the five other known compounds based on racemic combinations of Cu(phen)$_2$(H$_2$O)$^{2+}$ units to understand stacking motifs in these racemic compounds: [Cu(phen)$_2$(H$_2$O)][SO$_4$]·4H$_2$O (CSD refcode: MUNHUA),[9]

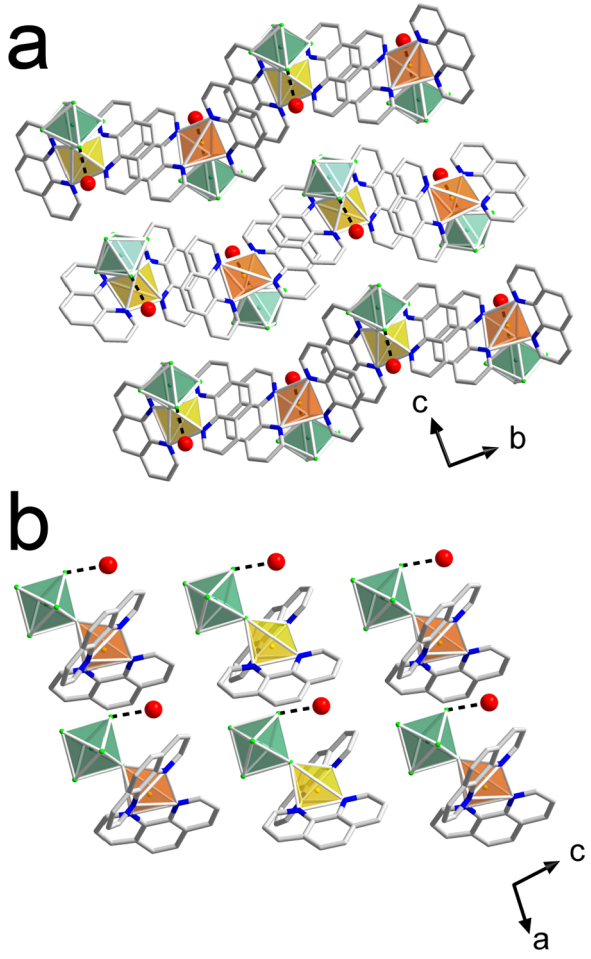

Figure 5. Structural diagram showing the face-to-face and parallel displaced stacking interactions in the structure of compounds **5** and **6**. (b) Hydrogen bonds within the structure are depicted as dashed lines. Orange polyhedra represent Λ-Cu(phen)$_2$(H$_2$O)$^{2+}$ cations, gold polyhedra represent Δ-Cu(phen)$_2$(H$_2$O)$^{2+}$ cations, and green polyhedra represent HfF$_6^{2-}$ anions.

[Cu(phen)$_2$(H$_2$O)][NO$_3$]$_2$ (CSD refcode: APENCU),[31] [Cu(phen)$_2$(H$_2$O)][ClO$_4$]$_2$ (CSD refcode: KOWFEH),[33] [Cu(phen)$_2$(H$_2$O)][BF$_4$]$_2$ (CSD refcode: APOLCU),[32] and [Cu(phen)$_2$(H$_2$O)][CF$_3$SO$_3$]$_2$ (CSD refcode: NEHXAZ).[33]

Stacking patterns in racemic Cu-phen compounds can be classified into three general categories: horizontal, zigzag, and diagonal. Horizontal stacking (shown in Figure 2) occurs when only face-to-face stacking interactions are present, as seen in compounds **1**−**4**. Zigzag configurations are found when both face-to-face and parallel displaced interactions are present in the same structure (Figure 5), as seen here in compounds **5** and **6** and in the known compound MUNHUA. Diagonal stacking (Figure 6) occurs when only parallel displaced stacking interactions are present and is observed in the known APENCU, KOWFEH, APOLCU, and NEHXAZ compounds listed above.

Diagonal and horizontal packed structures can be distinguished by the absence or presence of extended hydrogen-bonding networks, respectively. Hydrogen bonding in these structures is largely dependent on the charge of the anion. In Cu(phen)$_2$(H$_2$O)$^{2+}$ compounds with MF$_6^{2-}$ or SO$_4^{2-}$ anions, cations and anions are present in a 1:1 ratio. In contrast, compounds with NO$_3^-$, CF$_3$SO$_3^-$, BF$_4^-$, and ClO$_4^-$ anions

https://dx.doi.org/10.1021/acs.cgd.0c01355
Cryst. Growth Des. 2021, 21, 552−562

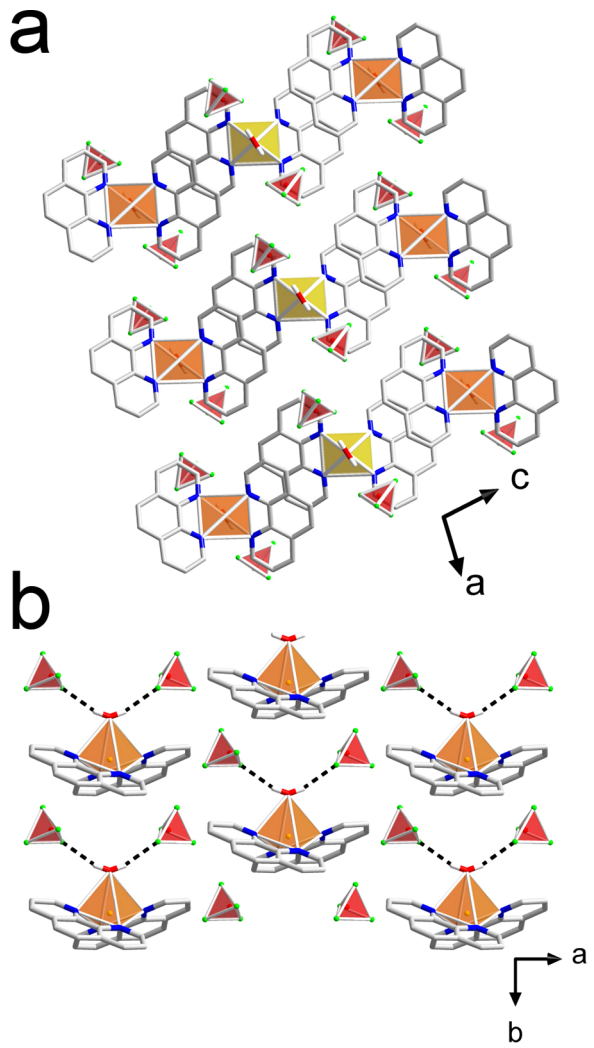

Figure 6. Structural diagram showing the parallel displaced stacking interactions in the structure of $[Cu(phen)_2(H_2O)][BF_4]_2$ (APOLCU) and other reported $Cu(phen)_2(H_2O)^{2+}$ compounds. (b) Hydrogen bonds within the structure are depicted as dashed lines. Orange polyhedra represent Λ-$Cu(phen)_2(H_2O)^{2+}$ cations, gold polyhedra represent Δ-$Cu(phen)_2(H_2O)^{2+}$ cations, and red polyhedra represent BF_4^- anions.

have a cation:anion ratio of 1:2. This distinction has profound consequences on the hydrogen bonding in the structure, which can be understood in terms of the numbers of hydrogen bond donors and acceptors present. In all known compounds that include $Cu(phen)_2(H_2O)^{2+}$, each bound water molecule participates in two hydrogen-bonding interactions. In compounds with a 1:1 cation:anion ratio, each anion participates in two hydrogen-bonding interactions with $Cu(phen)_2(H_2O)^{2+}$ units to fulfill the hydrogen-bonding preference of the apical bound water molecules on the cations, whereas in the 1:2 compounds each anion can only participate in one hydrogen-bonding interaction. The formation of $Cu(phen)_2(H_2O)^{2+}\cdots MF_6^{2-}\cdots Cu(phen)_2(H_2O)^{2+}$ clusters in the 1:1 compounds allows this condition to be satisfied. These clusters form between adjacent Δu−Λd−Δu−Λd and Δd−Λu−Δd−Λu stacking chains.

To distinguish zigzag packed structures from the horizontal and diagonal packing archetypes, the symmetry of the cation must also be considered. Just as the symmetry of the C_2-symmetric $Cu(phen)_2(H_2O)^{2+}$ complexes tends to be maintained in the stacking interactions of these cations (only face-to-face or only parallel displaced), the lower symmetry of C_1-symmetric $Cu(phen)_2MF_6$ complexes is reflected in their stacking interactions, with each phen ligand involved in a distinct stacking geometry (both face-to-face and parallel displaced in the same compound). In $Cu(phen)_2MF_6\cdot H_2O$ (M = Zr, Hf) and $[Cu(phen)_2(H_2O)][SO_4]\cdot 4H_2O$, the symmetry of the cation is reduced from C_2 to C_1 due to the tilting of the apical ligand toward the phen ligand that participates in face-to-face stacking. The tilting of the apical ligand is associated with distinct hydrogen-bonding interactions found in these compounds relative to the known Cu-phen racemates with horizontal or diagonal packing. For $Cu(phen)_2MF_6$ (M = Zr, Hf) units, the apical MF_6^{2-} group participates in a single hydrogen bond with a free water molecule (Figure 5). Similarly, in $[Cu(phen)_2(H_2O)][SO_4]\cdot 4H_2O$, the SO_4^{2-} group bridges between adjacent $Cu(phen)_2(H_2O)^{2+}$ cations, analogous to the bridging interactions found in the horizontal packed compounds, but in this case the bridging occurs through hydrogen bonding with a single oxide ligand rather than two fluoride ligands (Figure 7).

The dependence of stacking geometry in chiral Cu-phen complexes on molecular symmetry is well illustrated by $[Cu(phen)_2(SO_4)](H_2O)_2(dmf)$ (CSD refcode: MUNHOU) and $[Cu(phen)_2(SO_4)]CH_3OH$ (CSD refcode: MUNHIO). The structure of MUNHIO contains only parallel displaced

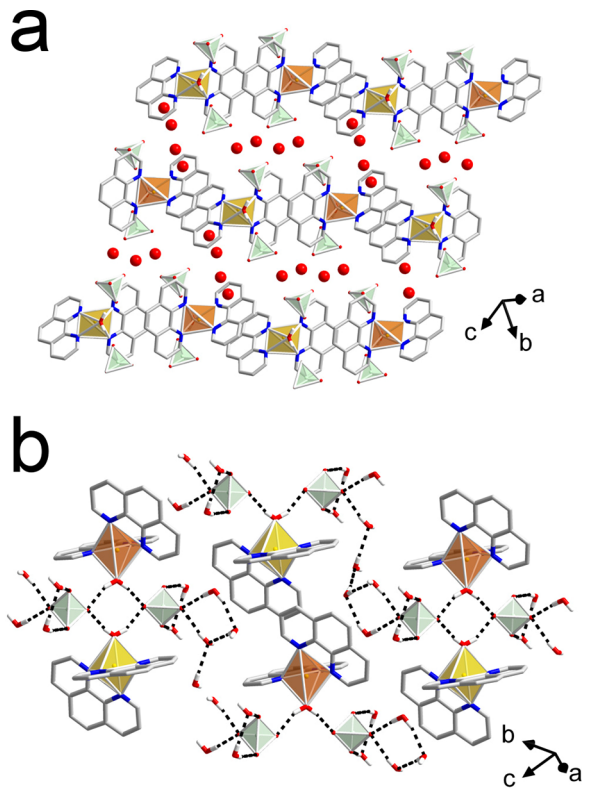

Figure 7. Structural diagram showing the face-to-face and parallel displaced stacking interactions in the structure of $[Cu(phen)_2(H_2O)][SO_4]\cdot 4H_2O$ (MUNHUA). (b) Hydrogen bonds within the structure are depicted as dashed lines. Orange polyhedra represent Λ-$Cu(phen)_2(H_2O)^{2+}$ cations, gold polyhedra represent Δ-$Cu(phen)_2(H_2O)^{2+}$ cations, and light green polyhedra represent SO_4^{2-} anions.

https://dx.doi.org/10.1021/acs.cgd.0c01355
Cryst. Growth Des. 2021, 21, 552−562

stacking interactions to give a diagonal stacking arrangement as $Cu(phen)_2(SO_4)$ molecules occupy 2-fold axes and retain C_2 symmetry, which is facilitated by symmetrical disorder of the apical SO_4^{2-} ligand. The symmetrical disorder is supported by the disorder of the solvating methanol molecule that occupies the same 2-fold axes, resulting in symmetrical hydrogen-bonding contacts between SO_4^{2-} and methanol. In contrast, although the apical SO_4^{2-} ligand is also disordered in MUNHOU, $Cu(phen)_2(SO_4)$ molecules in this compound participate in both face-to-face and parallel displaced stacking interactions to give a zigzag stacking arrangement. In this case, the ligand participates in hydrogen-bonding contacts with ordered hydrating water molecules to lower the symmetry of the $Cu(phen)_2(SO_4)$ molecule from C_2 to C_1.

Inversion Symmetry in Racemic $Cu(L)_2(H_2O)^{2+}$ (L = phen, bpy) Compounds. To elucidate how local $\pi-\pi$ stacking interactions contribute to the preservation or breaking of crystallographic inversion symmetry in racemic compounds, we compared the structures of compounds based on Δ- and Λ-$Cu(phen)_2(H_2O)^{2+}$ and Δ- and Λ-$Cu(bpy)_2(H_2O)^{2+}$ complexes. Although Δ- and Λ-$Cu(L)_2(H_2O)^{2+}$ (L = bpy, phen) units in these racemates participate in both homochiral and heterochiral $\pi-\pi$ stacking interactions, here we discuss only the heterochiral interactions, as these interactions can involve [redacted] (inversion, mirror/glide, rotoinversion) while homochiral stacking interactions cannot.

Whereas adjacent phen ligands are always parallel (displaced and face-to-face) when they are involved in stacking interactions between nearest-neighbor $Cu(phen)_2(H_2O)^{2+}$ complexes, parallel displaced, nonparallel displaced, and nonparallel face-to-face arrangements are observed between nearest neighbors for $Cu(bpy)_2(H_2O)^{2+}$ units. Nearest-neighbor $Cu(bpy)_2(H_2O)^{2+}$ complexes are related by inversion symmetry in $[Cu(bpy)_2(H_2O)][S_5O_6]$ (CSD refcode: BPACUS) and $[Cu(bpy)_2(H_2O)][S_2O_6]$ (CSD refcode: BPACUT), where $\pi-\pi$ stacking interactions are absent from the structure of BPACUS and parallel displaced stacking interactions are observed in BPACUT. Nonparallel configurations of bpy ligands in adjacent $Cu(bpy)_2(H_2O)^{2+}$ complexes preclude the possibility of inversion centers relating nearest neighbors that are opposite enantiomers. Nonparallel arrangements between nearest neighbors can lead to non-nearest neighbors being related only by glide planes, as observed in the $Cu(bpy)_2(H_2O)][MF_6]\cdot 3H_2O$ (M = Ti, Zr, Hf) family (CSD refcodes: YUGYEH, YUGYOR, YUGYIL), in which all stacking interactions are nonparallel and the structure is noncentrosymmetric.[21,24] In $[Cu(bpy)_2(H_2O)][BF_4]_2$ (CSD refcode: VIKDOJ) and $[Cu(bpy)_2(H_2O)][PF_6]_2$ (CSD refcode: EQIQOL), the $\pi-\pi$ stacking interaction is nonparallel with the nearest neighbor but parallel with the second nearest neighbor, giving rise to a centrosymmetric structure despite the noncentrosymmetric nonparallel local arrangement. In contrast, stacking interactions between $Cu(phen)_2(H_2O)^{2+}$ are always parallel, and heterochiral pairs are most commonly arranged across inversion centers.

The difference in stacking behavior between the racemic copper(II) complexes of phen and bpy may stem from the difference in available surface area. Previous studies of metal complexes of bpy and phen have shown that the $\pi-\pi$ interaction strength increases with increasing surface area, which suggests that stacking interactions between phen ligands are likely to be stronger than those between bpy ligands due to a larger surface area. In the case of strong stacking interactions between phen ligands, a parallel geometry allows for these interactions to be optimized. For bpy ligands, however, the weaker stacking interaction allows for other interactions in the structure to direct the packing landscape and can more easily bring the stacking geometry into a nonparallel configuration that can lead to broken local inversion symmetry.[29,30]

While the presence of nonparallel stacking between chiral $Cu(L)_2(H_2O)^{2+}$ (L = bpy, phen) complexes does not guarantee inversion symmetry breaking, nonparallel stacking reduces the number of possible configurations that lead to inversion symmetry. Local inversion symmetry is broken in the three known $Cu(L)_2(H_2O)^{2+}$ (L = bpy, phen) structures where nonparallel interactions are present between nearest neighbors, although the second-nearest neighbors are related by inversion in the VIKDOJ and EQIQOL structures. Thus, [redacted] interactions will lead to an increased likelihood of achieving an NCS structure in racemic compounds by breaking local inversion symmetry.

CONCLUSIONS

In this study, we report the structures of six novel racemic compounds based on complexes of copper(II) and 1,10-phenanthroline. Racemic combinations of C_2-symmetric Δ- and Λ-$Cu(phen)_2(H_2O)^{2+}$ cations found in $[Cu(phen)_2(H_2O)][TiF_6]\cdot H_2O$, $[Cu(phen)_2(H_2O)][HfF_6]\cdot xH_2O$, $[Cu(phen)_2(H_2O)][ZrF_6]\cdot 0.64H_2O$, and $[Cu(phen)_2(H_2O)][HfF_6]\cdot 0.87H_2O$ display only face-to-face $\pi-\pi$ stacking interactions, which gives rise to a horizontal packing arrangement that is unique among all known racemic $Cu(phen)_2(H_2O)^{2+}$ compounds. A comparison with previously reported racemic $Cu(phen)_2(H_2O)^{2+}$ compounds with [redacted] illustrates the key role of hydrogen bonding in determining the packing architectures in these compounds, as compounds without extended hydrogen-bonding networks are arranged via only parallel displaced stacking interactions. Cation symmetry was also found to strongly influence $\pi-\pi$ stacking interactions in $Cu(phen)_2ZrF_6\cdot H_2O$ and $Cu(phen)_2HfF_6\cdot H_2O$. Racemic combinations of Δ- and Λ-$Cu(phen)_2MF_6$ (M = Zr, Hf) complexes are arranged via both face-to-face and parallel displaced $\pi-\pi$ stacking interactions as a consequence of the tilting of the apical ligand, which lowers the local point group symmetry of the chiral species to C_1.

ASSOCIATED CONTENT

Supporting Information

The Supporting Information is available free of charge at https://pubs.acs.org/doi/10.1021/acs.cgd.0c01355.

Descriptors calculated to assign the geometry of $\pi-\pi$ stacking interactions (PDF)

Accession Codes

CCDC 2033377−2033382 contain the supplementary crystallographic data for this paper. These data can be obtained free of charge via www.ccdc.cam.ac.uk/data_request/cif, or by emailing data_request@ccdc.cam.ac.uk, or by contacting The Cambridge Crystallographic Data Centre, 12 Union Road, Cambridge CB2 1EZ, UK; fax: +44 1223 336033.

AUTHOR INFORMATION

Corresponding Author

Kenneth R. Poeppelmeier − *Northwestern University, Department of Chemistry, Evanston, Illinois 60208-3113,*

https://dx.doi.org/10.1021/acs.cgd.0c01355
Cryst. Growth Des. 2021, 21, 552−562

United States; orcid.org/0000-0003-1655-9127;
Email: krp@northwestern.edu

Authors

Matthew L. Nisbet − *Northwestern University, Department of Chemistry, Evanston, Illinois 60208-3113, United States;* orcid.org/0000-0001-9531-9193

Yiran Wang − *Northwestern University, Department of Chemistry, Evanston, Illinois 60208-3113, United States;* orcid.org/0000-0002-3642-2294

Complete contact information is available at: https://pubs.acs.org/10.1021/acs.cgd.0c01355

Notes

The authors declare no competing financial interest.

■ ACKNOWLEDGMENTS

This work was supported by funding from the National Science Foundation (DMR-1904701). Single-crystal X-ray diffraction data were acquired at IMSERC at Northwestern University, which has received support from the Soft and Hybrid Nanotechnology Experimental (SHyNE) Resource (NSF ECCS-1542205), the State of Illinois, and the International Institute for Nanotechnology (IIN).

■ REFERENCES

(1) Zhao, X.; Huang, S.; Liu, Y.; Li, J.; Zhu, W. Effects of noncovalent interactions on the impact sensitivity of HNS-based cocrystals: A DFT study. *Cryst. Growth Des.* **2019**, *19*, 756−767.

(2) Chen, T.; Li, M.; Liu, J. $\pi-\pi$ Stacking Interaction: A Nondestructive and Facile Means in Material Engineering for Bioapplications. *Cryst. Growth Des.* **2018**, *18*, 2765−2783.

(3) Datta, S.; Saha, M. L.; Stang, P. J. Hierarchical Assemblies of Supramolecular Coordination Complexes. *Acc. Chem. Res.* **2018**, *51*, 2047−2063.

(4) Steiner, T. The Hydrogen Bond in the Solid State. *Angew. Chem., Int. Ed.* **2002**, *41*, 48−76.

(5) Ye, B.-H.; Tong, M.-L.; Chen, X.-M. Metal-organic molecular architectures with 2,2′-bipyridyl-like and carboxylate ligands. *Coord. Chem. Rev.* **2005**, *249*, 545−565.

(6) Ma, Y.; Zhang, A.; Zhang, C.; Jiang, D.; Zhu, Y.; Zhang, C. Crystal Packing of Low-Sensitivity and High-Energy Explosives. *Cryst. Growth Des.* **2014**, *14*, 4703−4713.

(7) Lim, C.-S.; Jankolovits, J.; Kampf, J. W.; Pecoraro, V. L. Chiral Metallacrown Supramolecular Compartments that Template Nanochannels: Self-Assembly and Guest Absorption. *Chem. - Asian J.* **2010**, *5*, 46−49.

(8) Halasyamani, P. S.; Poeppelmeier, K. R. Noncentrosymmetric Oxides. *Chem. Mater.* **1998**, *10*, 2753−2769.

(9) Melnic, E.; Coropceanu, E. B.; Kulikova, O. V.; Siminel, A. V.; Anderson, D.; Rivera-Jacquez, H. J.; Masunov, A. E.; Fonari, M. S.; Kravtsov, V. C. Robust Packing Patterns and Luminescence Quenching in Mononuclear $[Cu(II)(phen)_2]$ Sulfates. *J. Phys. Chem. C* **2014**, *118*, 30087−30100.

(10) Kim, E.-a.; Lee, D. W.; Ok, K. M. Centrosymmetric $[N(CH_3)_4]_2TiF_6$ vs. noncentrosymmetric polar $[C(NH_2)_3]_2TiF_6$: A hydrogen-bonding effect on the out-of-center distortion of TiF_6 octahedra. *J. Solid State Chem.* **2012**, *195*, 149−154.

(11) Chen, C.; Wu, Y.; Li, R. The anionic group theory of the nonlinear optical effect and its applications in the development of new high-quality NLO crystals in the borate series. *Int. Rev. Phys. Chem.* **1989**, *8*, 65−91.

(12) Gautier, R.; Gautier, R.; Chang, K. B.; Poeppelmeier, K. R. On the Origin of the Differences in Structure Directing Properties of Polar Metal Oxyfluoride $[MO_xF_{6-x}]^{2-}$ (x = 1, 2) Building Units. *Inorg. Chem.* **2015**, *54*, 1712−1719.

(13) Jacques, J.; Collet, A.; Wilen, S. H. *Enantiomers, racemates, and resolutions*; Krieger: 1994.

(14) Hubbard, D. J.; Johnston, A. R.; Casalongue, H. S.; Sarjeant, A. N.; Norquist, A. J. Synthetic Approaches for Noncentrosymmetric Molybdates. *Inorg. Chem.* **2008**, *47*, 8518−8525.

(15) Veltman, T. R.; Stover, A. K.; Narducci Sarjeant, A.; Ok, K. M.; Halasyamani, P. S.; Norquist, A. J. Directed Synthesis of Noncentrosymmetric Molybdates Using Composition Space Analysis. *Inorg. Chem.* **2006**, *45*, 5529−5537.

(16) Gutnick, J. R.; Muller, E. A.; Narducci Sarjeant, A.; Norquist, A. J. $[C_5H_{14}N_2][(MoO_3)_3(SO_4)]\bullet H_2O$: Sulfated alpha-Molybdena Chains. *Inorg. Chem.* **2004**, *43*, 6528−6530.

(17) Glor, E. C.; Blau, S. M.; Yeon, J.; Zeller, M.; Shiv Halasyamani, P.; Schrier, J.; Norquist, A. J. $[R\text{-}C_7H_{16}N_2][V_2Te_2O_{10}]$ and $[S\text{-}C_7H_{16}N_2][V_2Te_2O_{10}]$; new polar templated vanadium tellurite enantiomers. *J. Solid State Chem.* **2011**, *184*, 1445−1450.

(18) Muller, E. A.; Cannon, R. J.; Sarjeant, A. N.; Ok, K. M.; Halasyamani, P. S.; Norquist, A. J. Directed Synthesis of Noncentrosymmetric Molybdates. *Cryst. Growth Des.* **2005**, *5*, 1913−1917.

(19) Guerin, S.; O'Donnell, J.; Haq, E. U.; McKeown, C.; Silien, C.; Rhen, F. M. F.; Soulimane, T.; Tofail, S. A. M.; Thompson, D. Racemic Amino Acid Piezoelectric Transducer. *Phys. Rev. Lett.* **2019**, *122*, 047701.

(20) Dalhus, B.; Görbitz, C. H. Non-centrosymmetric racemates: space-group frequencies and conformational similarities between crystallographically independent molecules. *Acta Crystallogr., Sect. B: Struct. Sci.* **2000**, *56*, 715−719.

(21) Gautier, R.; Norquist, A. J.; Poeppelmeier, K. R. From Racemic Units to Polar Materials. *Cryst. Growth Des.* **2012**, *12*, 6267−6271.

(22) Breu, J.; Domel, H.; Stoll, A. Racemic Compound Formation versus Conglomerate Formation with $[M(bpy)_3](PF_6)_2$ (M = Ni, Zn, Ru); Molecular and Crystal Structures. *Eur. J. Inorg. Chem.* **2000**, *2000*, 2401−2408.

(23) Breu, J.; Domel, H.; Norrby, P.-O. Racemic Compound Formation versus Conglomerate Formation with $[M(bpy)_3](PF_6)_2$ (M = Ni, Zn, Ru); Lattice Energy Minimisations and Implications for Structure Prediction. *Eur. J. Inorg. Chem.* **2000**, *2000*, 2409−2419.

(24) Nisbet, M. L.; Pendleton, I. M.; Nolis, G. M.; Griffith, K. J.; Schrier, J.; Cabana, J.; Norquist, A. J.; Poeppelmeier, K. R. Machine-Learning-Assisted Synthesis of Polar Racemates. *J. Am. Chem. Soc.* **2020**, *142*, 7555−7566.

(25) Bersuker, I. B. Pseudo-Jahn−Teller Effect—A Two-State Paradigm in Formation, Deformation, and Transformation of Molecular Systems and Solids. *Chem. Rev.* **2013**, *113*, 1351−1390.

(26) Gautier, R.; Poeppelmeier, K. R. Preservation of Chirality and Polarity between Chiral and Polar Building Units in the Solid State. *Inorg. Chem.* **2012**, *51*, 10613−10618.

(27) Hunter, C. A.; Sanders, J. K. M. The nature of.pi.-.pi. interactions. *J. Am. Chem. Soc.* **1990**, *112*, 5525−5534.

(28) Hunter, C. A. Quantifying Intermolecular Interactions: Guidelines for the Molecular Recognition Toolbox. *Angew. Chem., Int. Ed.* **2004**, *43*, 5310−5324.

(29) Janjić, G. V.; Petrović, P. V.; Ninković, D. B.; Zarić, S. D. Geometries of stacking interactions between phenanthroline ligands in crystal structures of square-planar metal complexes. *J. Mol. Model.* **2011**, *17*, 2083−2092.

(30) Petrović, P. V.; Janjić, G. V.; Zarić, S. D. Stacking Interactions between Square-Planar Metal Complexes with 2,2′-Bipyridine Ligands. Analysis of Crystal Structures and Quantum Chemical Calculations. *Cryst. Growth Des.* **2014**, *14*, 3880−3889.

(31) Nakai, H.; Deguchi, Y. The Crystal Structure of Monoaquobis(1,10-phenanthroline)copper(II) Nitrate, $[Cu(H_2O)(phen)_2](NO_3)_2$. *Bull. Chem. Soc. Jpn.* **1975**, *48*, 2557−2560.

(32) Nakai, H.; Noda, Y. The Crystal Structure of Monoaquabis(1,10-phenanthroline)copper(II) Tetrafluoroborate $[Cu(H_2O)(phen)_2](BF_4)_2$. *Bull. Chem. Soc. Jpn.* **1978**, *51*, 1386−1390.

(33) Murphy, G.; Murphy, C.; Murphy, B.; Hathaway, B. Crystal structures, electronic properties and structural pathways of two[Cu-

$(phen)_2(OH_2)][Y]_2$ complexes(phen = 1,10-phenanthroline,Y = $CF_3SO_3^-$ or ClO_4^-). *J. Chem. Soc., Dalton Trans.* **1997**, 2653−2660.
(34) Harrison, W. T. A.; Nenoff, T. M.; Gier, T. E.; Stucky, G. D. Tetrahedral-atom 3-ring groupings in 1-dimensional inorganic chains: beryllium arsenate hydroxide hydrate ($Be_2AsO_4OH \cdot 4H_2O$) and sodium zinc hydroxide phosphate hydrate ($Na_2ZnPO_4OH \cdot H_2O$). *Inorg. Chem.* **1993**, *32*, 2437−2441.
(35) *SAINT V8.38A*; Bruker Analytical X-ray Instruments: Madison, WI, USA. 2016.
(36) Sheldrick, G. M. *SADABS*; University of Göttingen: Göttingen, Germany, 2002.
(37) *CrysAlisPro*; Rigaku Oxford Diffraction/Agilent Technologies UK Ltd: Yarnton, England, 2019.
(38) Sheldrick, G. M. Crystal structure refinement with SHELXL. *Acta Crystallogr., Sect. C: Struct. Chem.* **2015**, *71*, 3−8.
(39) Dolomanov, O. V.; Bourhis, L. J.; Gildea, R. J.; Howard, J. a. K.; Puschmann, H. OLEX2: a complete structure solution, refinement and analysis program. *J. Appl. Crystallogr.* **2009**, *42*, 339−341.
(40) Spek, A. L. Single-crystal structure validation with the program PLATON. *J. Appl. Crystallogr.* **2003**, *36*, 7−13.
(41) Groom, C. R.; Bruno, I. J.; Lightfoot, M. P.; Ward, S. C. The Cambridge Structural Database. *Acta Crystallogr., Sect. B: Struct. Sci., Cryst. Eng. Mater.* **2016**, *72*, 171−179.
(42) Donakowski, M. D.; Gautier, R.; Yeon, J.; Moore, D. T.; Nino, J. C.; Halasyamani, P. S.; Poeppelmeier, K. R. The Role of Polar, Lamdba (Λ)-Shaped Building Units in Noncentrosymmetric Inorganic Structures. *J. Am. Chem. Soc.* **2012**, *134*, 7679−7689.

https://dx.doi.org/10.1021/acs.cgd.0c01355
Cryst. Growth Des. 2021, 21, 552−562